ACS MATERIALS LETTERS

www.acsmaterialsletters.org

LETTER

Determining Optical Band Gaps of MOFs

Kevin Fabrizio, Khoa N. Le, Anastasia B. Andreeva, Christopher H. Hendon,* and Carl K. Brozek*

Cite This: *ACS Materials Lett.* 2022, 4, 457–463

Read Online

ACCESS | Metrics & More | Article Recommendations | Supporting Information

ABSTRACT: **Assigning optical band gaps to MOFs is paramount for understanding their optical, electronic, and reactivity properties, but literature reports have produced a wide range of values for even the same MOF. Despite the molecular nature of MOF electronic structures, experimental assignments employ Tauc analysis, a method applied to semiconductors. Here, we report optical band gaps of common MOFs and demonstrate that Gaussian fitting is more appropriate for assigning accurate gap energies. We further support this claim with DFT simulation, providing a reliable method for estimating optical band gaps from ground-state hybrid-GGA. MOFs that require Tauc analysis exhibit overlapping optical transitions uncommon for typical carboxylate-based MOFs and more akin to narrow-gap semiconductors. Taken together, these results provide a simple roadmap for assigning MOF optical band gaps.**

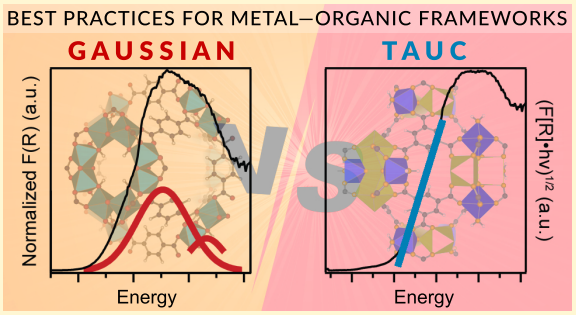

Downloaded via UNIV OF OREGON on February 4, 2022 at 18:07:51 (UTC).
See https://pubs.acs.org/sharingguidelines for options on how to legitimately share published articles.

Electronic fundamental gaps (or electronic band gaps in solids, HOCO-LUCO gaps in molecular crystals, and HOMO–LUMO gaps in molecules, E_g) define the difference in energy between the highest filled orbital (valence band) and lowest empty orbital (conduction band) of a material. Measuring the electronic band gap of a material is important for understanding its redox, optical, and electronic properties.[1−4] Optical band gaps (E_{opt}), hereafter termed optical gaps, on the other hand, refer to the photon energy required to access the lowest-energy optically excited state.[5] In comparison to the electronic band gap, the energy of the optical gap is reduced due to the stabilizing interaction between the photogenerated hole and electron, termed the exciton binding energy (E_b). When exciton binding energies are small in comparison to the band gap, E_{opt} serves as a useful approximation for the E_g, for example as in bulk CdSe E_b = 15 meV, with E_g = 1.66 eV.[6−8] However, E_{opt} becomes comparable to E_b in chemical systems with more localized binding, such as organic polymers and molecules. For example, polythiophene has an E_b of 0.6 eV, anthracene exhibits an E_b of 1.0 eV, and MOF-5 was recently estimated to have E_b = 3.5 eV.[9−11] In such molecular-type systems, the E_{opt} substantially underestimates the band gap, but E_g may be obtained by photoelectron spectroscopy, or estimated using a DFT-based quasiparticle perturbation theory (e.g., G_0W_0),[12,13] instead. Knowing the optical gaps of materials, on the other hand, is critical for harnessing the photophysical properties of materials to design devices for photocatalysis, solar energy conversion, optical sensors, and display technologies, where excitonic interactions become relevant. Assigning optical gaps poses significant challenges, however, especially for materials with localized, molecular-type bonding.

In general, optical gaps of materials are determined from optical absorption spectroscopy, but data analysis depends on the electronic structures and, hence, the bonding characteristics of the material. Methods generally fall into two categories: (1) peak fitting or (2) Tauc analysis. In the former, the peak position of the lowest-energy optical transition is determined by fitting a spectrum to Gaussian band-shapes or by locating the zero-crossing-point of the derivative of the spectrum. These methods find widespread use across spectroscopy involving well-resolved band-shapes, such as electron paramagnetic resonance or photoluminescence spectroscopies.[14−16] Accordingly, optical absorption spectra of materials with molecular-type electronic structures are amenable to these methods because the discrete transitions between a sparse density of states (DOS) produce spectra with well-resolved peak positions. For example, analysis of quantum dot and perovskite spectra relies on Gaussian fittings due to the quantum-confined electronics of quantum dots and the highly ionic bonding of perovskites.[17−19] On the other hand, in typical semiconductors and amorphous materials, numerous overlapping transitions complicate Gaussian fitting.[20] In such cases, spectra are interpreted by Tauc analysis, with the spectra replotted as $(\alpha h\nu)^{1/n}$ versus photon energy, where α refers to the absorption coefficient of the material, $h\nu$ is the photon

Received: December 28, 2021
Accepted: January 25, 2022

© XXXX American Chemical Society

https://doi.org/10.1021/acsmaterialslett.1c00836
ACS Materials Lett. 2022, 4, 457–463

energy, and the exponent $1/n$ denotes the nature of the optical transition, with $n = 1/2$ for direct allowed transitions, $n = 3/2$ for direct forbidden transitions, $n = 2$ for indirect allowed transitions, and $n = 3$ for indirect forbidden transitions.[20] Typically, the region with the highest slope is fitted to a line and the intersection of the line with the abscissa (i.e., photon energy) is taken as the optical gap. Conventional semiconductors, such as Si and Ge, and defective materials with a high concentration of midgap states, require Tauc analysis.[20,21] Unlike in molecular-type systems where a well-resolved band clearly defines the optical gap, the onset of absorption defines the optical gap because defects and covalent bonding (dispersive bands) give rise to numerous transitions with comparable intensities. Figure 1 compares hypothetical sets of data where, on one hand, flat band curvature permits facile Gaussian fitting, while the other example involves numerous overlapping Gaussian peaks due to dispersive electronic bands, necessitating Tauc analysis.

Metal−organic frameworks (MOFs) pose a fundamental challenge to assigning optical gaps because, despite being extended solids, the vast majority of examples comprise of molecular-building blocks with highly localized bonding interactions. To our knowledge, few, if any, photoelectron experiments have been reported for common MOFs as direct experimental measurement of MOF electronic band gaps. In other words, estimating E_b remains elusive. Yet, computational studies of common MOFs, such as MOF-5, suggest the optical gap to be nearly half of the electronic band gap,[10] implying that optical gaps obtained from spectroscopy vastly underestimate electronic band gaps. While knowing E_g facilitates the understanding of MOF reactivity and electrochemical properties, harnessing their photophysical properties and gaining insight into their excitonic interactions requires proper assignment of MOF optical gaps.

Yet, even for common MOFs, optical gaps remain disputed in the literature. In general, literature reports employ Tauc analysis to analyze the optical absorption spectra of MOFs, giving rise to optical gaps that vary by more than 1 eV, likely because of discrepancies between linear fits. For example, reported "band gaps" (used interchangeably with optical gap) of ZIF-8 (Zn-(imidazolate)$_2$) vary between 3.87 and 5.45 eV,[22−24] UiO-66 ($Zr_6O_4(OH)_4$(terephthalate)$_{12}$) vary between 2.50 and 4.07 eV,[25−27] and MIL-125 ($Ti_8O_8(OH)_4$(terephthalate)$_6$) range from 3.1 to 4.62 eV.[28−31] Furthermore, calculated electronic band structures indicate most MOFs possess localized bonding, with discrete, nonoverlapping states.[32] Given their molecular, rather than band-type, nature as well as the empirical observation that experimental spectra bear well-resolved peaks, suggests that MOFs should be well-suited to Gaussian peak-fitting, *not Tauc analysis*, to obtain optical gaps.

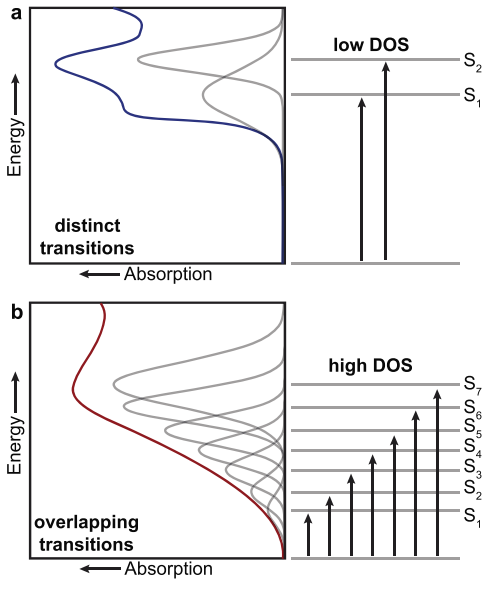

Figure 1. Hypothetical absorption spectra with Gaussian fits and state diagrams for (a) a material with flat band curvature and (b) a material with high band curvature requiring Tauc analysis.

Here, we report experimental optical spectra of common MOF materials and propose a standard procedure for assigning MOF optical gaps using experiment and/or computation. Specifically, we propose that Gaussian fittings serve as the appropriate method to assign optical gaps to the vast majority of MOFs unless the MOF possesses numerous overlapping transitions bands, as in systems with open-shell transition metals and dispersive bands, such as materials with strongly covalent metal−ligand bonds. Furthermore, we present a reliable ground-state DFT approach to examine the DOS at the band edges and predict the optical gaps of common MOFs. Comparison of experiment and theory suggests that assigning gaps with Gaussians serves as a simple approach that requires the least insight into the electronic structure and consistently shows agreement with DFT-computed gaps within 30 meV, on average. These guidelines radically alter the conventional approach to understanding MOF electronic structures and serve as quick methods for ascertaining optical, not electronic band gaps.

To determine the appropriate method for assigning MOF optical gaps, UV−vis−NIR diffuse reflectance spectra were collected on a representative collection of common MOFs. These include materials with open d-shell transition metal ions, such as Cu_3(benzenetricarboxylate)$_2$ (Cu-HKUST-1) and Cu(1,2,3-triazolate)$_2$ (Cu(ta)$_2$), materials with closed d-shell transition metal ions, such as Zn(imidazolate)$_2$ (ZIF-8), and materials with nontransition metals, such as Mg_2(2,5-dioxido-1,4-benzenedicarboxylate) (Mg-MOF-74). The spectra of all MOFs were transformed as the Kubelka−Munk function and are shown in Figures S13−25. To assign the optical gaps, all spectra were analyzed by three methods: Gaussian fitting, derivative analysis, and from Tauc plots. Details of these methods are described in the Supporting Information. In short, Gaussian analysis involved an initial guess of the absorption maximum prior to algorithmic fitting and Gaussians were allowed to shift in location, height, and width. The final number of Gaussians was chosen to minimize residuals and the optical gap was determined as the peak position of the lowest-energy Gaussian. In derivative analysis, a derivative was taken of the spectra and the optical gap was chosen as the lowest-energy photon energy where the derivative crosses zero. In Tauc analysis, the reflectance values plotted as the Kubelka−Munk function ($F(R)$) were treated as the absorption coefficient, and all spectra were plotted with both $n = 2$ and $n = 1/2$ to evaluate them as either indirect- or direct-gap materials. The Tauc analysis of several MOF materials, such as in MIL-53(Fe) and Cu-HKUST-1, required multiple linear fits to distinct linear regions. In such cases, the optical gaps derived from all linear fits were considered in comparison to theory.

https://doi.org/10.1021/acsmaterialslett.1c00836
ACS Materials Lett. 2022, 4, 457−463

Table 1. Summary of MOFs with Optical Gaps Determined by Experiment and DFT Simulations[a]

MOF name	organic ligand	metals	direct/indirect	DFT E_{opt}	Gaussian E_{opt}	Tauc direct E_{opt}	Tauc indirect E_{opt}
MOF-5	terephthalate	Zn	indirect	4.64	**4.71**	5.26	3.71
MIL-125	terephthalate	Ti	direct	3.87	**3.88**	4.02	3.68
UiO-66	terephthalate	Zr	direct	4.14	**4.26**	4.01	3.91
Mg-MOF-74	terephthalate	Mg	indirect	2.89	**2.86**	2.75	2.60
MIL-53(Fe)	terephthalate	Fe	indirect	2.28	**2.35**	2.93	2.01
PCN-415	terephthalate	Ti, Zr	direct	3.15	3.76	3.51	**3.25**
Cu-HKUST-1	trimesate	Cu	direct AFM	3.82	3.17	**3.38**	2.24
MUV-10(Ca)	trimesate	Ca	direct	4.22	**4.23**	4.06	3.70
MUV-10(Mn)	trimesate	Mn	indirect	2.98	4.52	3.91	**3.04**
$Cu(ta)_2$	1,2,3-triazolate	Cu	indirect AFM	3.20	4.06	3.69	**3.35**
ZIF-8	1-methylimidazolate	Zn	direct	5.32	**5.35**	5.36	5.17
MFM-300(Sc)	biphenyl-3,3′,5,5′′-tetracarboxylate	Sc	indirect	3.95	**4.00**	3.83	3.69
SU-101(Bi)	ellagate	Bi	indirect	2.34	2.45	2.76	**2.39**

[a]E_{opt} reported in eV, and values highlighted in bold indicate the E_{opt} with the lowest % difference. All spectra, subsequent fittings, and residuals are shown in **S13−25**. AFM signifies that the antiferromagnetically coupled configuration was simulated.

Table 2. Comparison of Optical Gaps Determined from Experiment and DFT[a]

MOF name	ΔE_{opt} Tauc direct	ΔE_{opt} Tauc indirect	ΔE_{opt} Gaussian	% difference Tauc direct	% difference Tauc indirect	% difference Gaussian
MOF-5	0.62	0.93	**0.07**	13.4	20.0	**1.51**
MIL-125	0.15	0.19	**0.005**	3.88	4.91	**0.13**
UiO-66	0.13	0.230	**0.12**	3.14	5.56	**2.90**
Mg-MOF-74	0.20	0.29	**0.03**	4.84	10.0	**1.04**
MIL-53(Fe)	0.65	0.27	**0.07**	28.5	11.8	**3.07**
PCN-415	0.36	**0.10**	0.61	11.4	**3.17**	19.4
Cu-HKUST-1	**0.44**	1.58	0.65	**11.5**	41.3	17.0
MUV-10(Ca)	0.16	0.52	**0.01**	3.79	12.3	**0.24**
MUV-10(Mn)	0.93	**0.06**	1.54	31.2	**2.01**	51.7
$Cu(ta)_2$	0.49	**0.15**	0.86	13.3	**4.48**	21.1
ZIF-8	0.04	0.15	**0.02**	0.75	2.82	**0.36**
MFM-300(Sc)	0.12	0.26	**0.05**	3.04	6.58	**1.27**
SU-101(Bi)	0.42	**0.05**	0.11	17.9	**2.14**	4.70

[a]ΔE_{opt} reported in eV and calculated as the difference between E_{opt} (DFT) and E_{opt} (experimental). % Difference is calculated as $|1 - E_{opt}(DFT)/E_{opt}(experimental)|$. Values highlighted in bold indicate the E_{opt} with the lowest % difference.

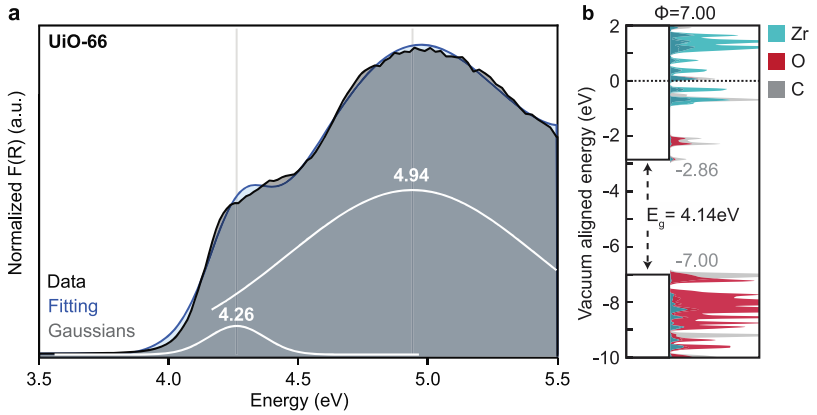

Figure 2. Analysis of UiO-66 optical spectra. (a) Diffuse reflectance UV−vis data with Gaussian fits and (b) computed DOS aligned to the vacuum level using the method detailed in ref 31.

To determine the nature of the optical transitions, that is, direct or indirect, we employed hybrid density functional theory (DFT) calculations because many hybrid functions (e.g., HSE06, B3LYP, M06, etc.) tend to underestimate the true electronic band gap and instead match experimental optical gaps by design. Specifically, unlike Hartree−Fock methods, DFT computes the energies of LUMOs (conduction bands) in the presence of $n-1$ electrons and, when combined with a portion of exact exchange, the functionals approximate the electron−hole attraction, that is, the exciton binding energy.[33] Because the vast majority of MOFs are thought to possess localized electronic states,[32] hybrid DFT serves as an accurate estimate of MOF optical gaps, and should fail to recover the true electronic band gap if E_b is large. Indeed, Poloni and colleagues calculated a gap of ∼4.5 eV for MOF-5 from hybrid DFT, which matched the experimentally

https://doi.org/10.1021/acsmaterialslett.1c00836
ACS Materials Lett. 2022, 4, 457−463

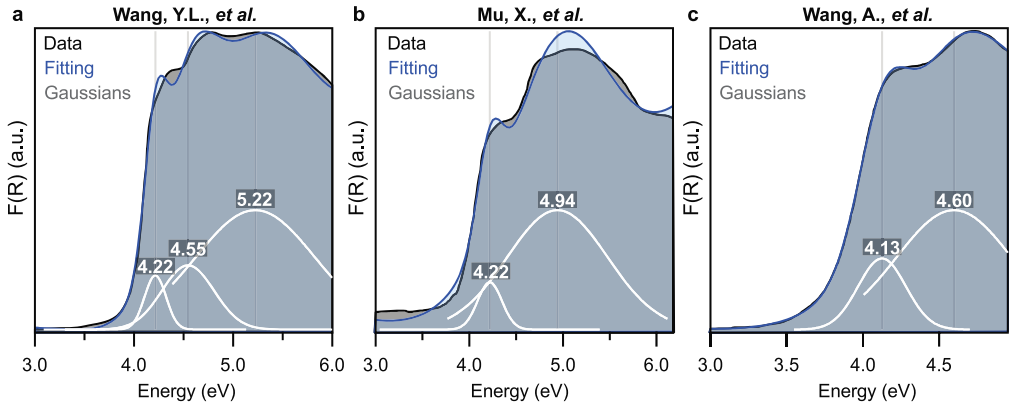

Figure 3. Gaussian-fitted diffuse-reflectance UV−vis data for UiO-66 digitized from (a) Wang et al. (ref 27), (b) Mu, X (ref 45), and (c) Wang et al. (ref 46).

determined optical gap, but estimated the exciton binding energy to be ∼3.5 eV from GW perturbation theory, suggesting the true electronic band gap of MOF-5 to be ∼8 eV.[10] Because of the great expense of GW-methods and because of the practical utility of estimating E_{opt} for understanding MOF photophysical properties, we employed relatively inexpensive hybrid-GGA approaches, in particular the tightly converged HSE06/HSEsol06 functional (see Supporting Information for computational methods) because of its broad implementation in standard quantum chemical software packages. Furthermore, this level of DFT theory has been shown to yield remarkable agreement with experimental optical gaps,[34] especially in MOFs.[32,35]

Table 1 summarizes optical gaps and the nature of the optical transitions determined by DFT, and experimental optical gaps determined from Tauc, Gaussian, and derivative analysis for a set of common MOFs. Although the vast majority of MOFs involve closed-shell metal ions, such as Mg^{2+} or Zn^{2+},[36−38] this collection overrepresents the share of open-shell systems because we deliberately sought MOFs that would test the limits of Gaussian analysis. Table 2 shows the absolute difference between the experimental and DFT-computed values (E_{diff}), and as the percentage difference ($E_{\%}$), defined as |1 − (experimental gap/DFT gap)|. For most MOFs, Gaussian fitting shows good agreement with DFT, with E_{diff} of 150 meV or less and $E_{\%}$ of 5% or less for most systems. In general, the MOFs most suited to analysis by Gaussian fittings contained alkali Earth metals, such as Mg^{2+}, as in Mg-MOF-74, closed-shell metal ions, such as Zn^{2+}, as in ZIF-8, or d^0 metal ions, such as Zr^{4+} in UiO-66. Derivative analysis, overall, showed worse agreement with DFT than Gaussian fits, suggesting it is less accurate at determining the position of individual transitions. Figure 2a shows the experimental spectrum for UiO-66 analyzed by Gaussian fits that provide a clear peak maxima in good agreement with DFT (both the fundamental gap E_g 4.14 eV matches the E_{opt} = 4.26 eV, and the second absorption feature measured at 4.96 eV corresponds to the DOS at ∼2.25 eV below the vacuum level), despite prior literature reporting a range of UiO-66 band gaps extracted from Tauc plots.[25−27,39−41]

As reflected in the conduction band DOS of UiO-66, Figure 2b, most MOFs exhibit discretely spaced frontier orbitals, making them better suited to Gaussian peak fitting. To examine the applicability of Gaussian analysis to experimental spectra reported elsewhere and to compare our E_{opt} values to literature reports, we applied Gaussian band-shapes to several previously reported spectra of UiO-66, MOF-5, and MIL-125.[27,42−46] Figure 3 shows data digitized from three distinct reports of UiO-66 with our fits. Gaussian fits in panels a, b, and c give E_{opt} of 4.22, 4.22, and 4.13 eV, all in excellent agreement with the DFT-predicted value of 4.14 eV, and our measured value of 4.26 eV shown in Figure 2. In comparison, the reported Tauc analysis gave values of 3.82, 3.91, and 3.45 eV, respectively.[27,45,46] These results suggest that even for MOFs, such as UiO-66, prone to midgap states (attributed to surface-bound or missing-linker defects) that lead to significant Urbach tailing, Gaussian fitting provides a facile technique for identifying absorption maxima in MOFs that can be attributed to the optical gap. Similar analysis of data digitized for MOF-5 and MIL-125 (Figures S26−27) gave E_{opt} values agree with our DFT-computed values, suggesting this technique is generally applicable to MOFs with distinct absorption features.

This analysis indicates that a subset of MOFs shows better agreement with Tauc analysis if they possess closely spaced excited states due to dispersive band curvatures, partially filled d-orbitals giving rise to multiple d−d transitions, as in $Cu(ta)_2$, covalent metal−ligand bonding, as in SU-101(Bi), or overlapping ligand-field transitions, as in MUV-10(Mn). For example, Figure 4a shows the experimental spectrum of MUV-10(Mn) and the attempted Gaussian fitting. Because of the numerous overlapping transitions, as corroborated by the DOS diagram shown in Figure 4c, Tauc analysis is more appropriate, as shown in Figure 4b. Similarly, Tauc should be considered for conductive MOFs because of the curvature of their band structures, which produce numerous overlapping optical transitions.[47] Although PCN-415 is computed to be a direct-gap material, its spectra showed better agreement with an indirect-gap ($E_{\%}$ of 3.14% vs 11.4%, respectively, Figure S23). Because calculations predict a valence band dispersion of only ∼2 meV for PCN-415, we suspect this discrepancy arises from numerous indirect-gap transitions becoming thermally activated at room temperature. Therefore, while Gaussian fitting is appropriate for typical MOF materials, the onset of absorption determined by Tauc analysis might still prove useful for investigations into the presence of midgap states that give rise to absorption "tails" and to the limited set of MOFs with dispersive band-type electronic structures. For example, Gaussian analysis of UiO-66 materials with varying defect concentrations still permits identification of the optical band gap, whereas the onset of absorption can be independently determined by Tauc fitting, and additional Gaussian bands can

https://doi.org/10.1021/acsmaterialslett.1c00836
ACS Materials Lett. 2022, 4, 457−463

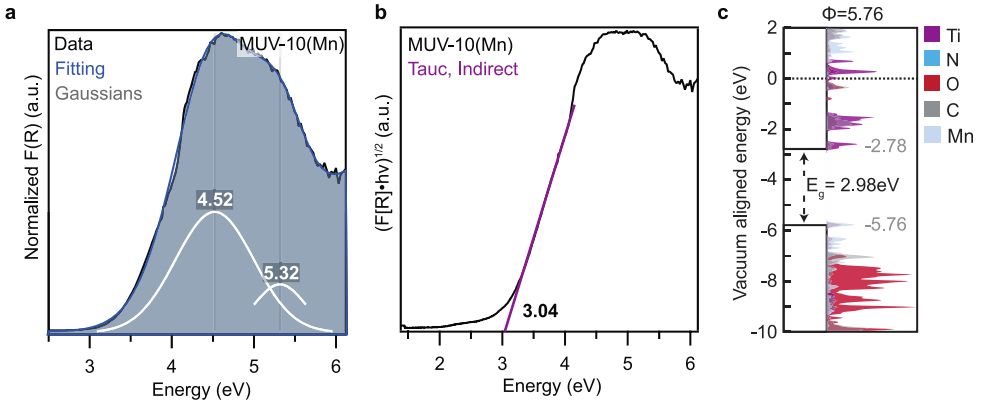

Figure 4. Analysis of MUV-10(Mn) optical spectra. (a) Diffuse reflectance UV−vis data and corresponding Gaussian fits, (b) Tauc plot and linear fit, and (c) computed DOS and band alignment.

be used to identify the position of discrete midgap states (Figure S28).

On the basis of these comparisons, we offer the following recommendations for assigning optical gaps to MOFs:

1. From the computed electronic band structure and corresponding DOS, determine the nature of the transition, use the appropriate Tauc fitting, and compare the results to values from Gaussian fits, as demonstrated here.
2. If full band diagram calculations of a MOF are not available, fit experimental data to Gaussians.
3. If working with MOFs that contain highly covalent metal-linker bonds, as in MOFs with nitrogen, sulfur, carbon-containing atoms bound to the metal, consider Tauc, but compare to Gaussian fits. If a peak maximum is clearly seen at the lowest-energy portion of the spectrum, likely use Gaussian fits.
4. If working with MOFs that contain transition metal ions with partially filled d-blocks, consider Tauc. If a peak maximum is clearly seen at the lowest-energy portion of the spectrum, likely use Gaussian fittings.
5. If working with MOFs that contain a high concentration of missing metal/linker defects, structural disorder, or midgap states, consider Tauc to identify the onset of absorption. Gaussian fitting, however, can still prove useful in independently determining the position of discrete midgap states and the position of E_{opt} of the pristine material.

In conclusion, this combined experimental-computational study reports the optical gaps of common MOFs through several experimental methods and by DFT calculations. In general, Gaussian fits to experimental reflectance spectra show greatest agreement with DFT-derived optical gaps, owing to the localized bonding found in most MOFs. For a subset of MOFs, such as systems with partially filled d-orbitals, Tauc analysis produced greater agreement, which we attribute to the greater number of overlapping optical transitions that impede Gaussian fitting. Overall, these results justify a set of recommendations for using simple methods to report the optical band gaps of MOFs.

■ ASSOCIATED CONTENT

Supporting Information

The Supporting Information is available free of charge at https://pubs.acs.org/doi/10.1021/acsmaterialslett.1c00836.

MOF experimental procedures and characterization, DRUV−vis spectra, Gaussian fittings, Tauc fittings, computational methods, and PDOSs (PDF)

■ AUTHOR INFORMATION

Corresponding Authors

Christopher H. Hendon − *Department of Chemistry and Biochemistry, Material Science Institute, University of Oregon, Eugene, Oregon 97403, United States;* orcid.org/0000-0002-7132-768X; Email: chhendon@uregon.edu; pages.uoregon.edu/chendon/

Carl K. Brozek − *Department of Chemistry and Biochemistry, Material Science Institute, University of Oregon, Eugene, Oregon 97403, United States;* orcid.org/0000-0002-8014-7904; Email: cbrozek@uoregon.edu, brozeklab.uoregon.edu

Authors

Kevin Fabrizio − *Department of Chemistry and Biochemistry, Material Science Institute, University of Oregon, Eugene, Oregon 97403, United States;* orcid.org/0000-0001-9700-1824

Khoa N. Le − *Department of Chemistry and Biochemistry, Material Science Institute, University of Oregon, Eugene, Oregon 97403, United States*

Anastasia B. Andreeva − *Department of Chemistry and Biochemistry, Material Science Institute, University of Oregon, Eugene, Oregon 97403, United States*

Complete contact information is available at: https://pubs.acs.org/10.1021/acsmaterialslett.1c00836

Notes

The authors declare no competing financial interest.

■ ACKNOWLEDGMENTS

We gratefully acknowledge the University of Oregon for startup funds. This work made use of the CAMCOR facility of the Lorry I. Lokey Laboratories at the University of Oregon to perform VT-DRUV−vis experiments. This material is based upon work supported by the National Science Foundation through the Division of Materials Research under Grant DMR-1956403 and through the Department of Energy through the Office of Basic Energy Sciences under Grant DE-SC0022147. C.H.H. acknowledges the Research Corporation for Science Advances (Cottrell Award). We also acknowledge the

https://doi.org/10.1021/acsmaterialslett.1c00836
ACS Materials Lett. 2022, 4, 457−463

continued support from the Extreme Science and Engineering Discovery Environment (XSEDE), which is supported by the National Science Foundation (ACI-1548562) and the PICS Coeus High Performance Computer, which is supported by the National Science Foundation (1624776).

REFERENCES

(1) Lin, K.-F.; Cheng, H.-M.; Hsu, H.-C.; Lin, L.-J.; Hsieh, W.-F. Band Gap Variation of Size-Controlled ZnO Quantum Dots Synthesized by Sol−Gel Method. *Chem. Phys. Lett.* **2005**, *409*, 208−211.

(2) Khatun, N.; Rini, E. G.; Shirage, P.; Rajput, P.; Jha, S. N.; Sen, S. Effect of Lattice Distortion on Bandgap Decrement Due to Vanadium Substitution in TiO_2 Nanoparticles. *Mater. Sci. Semicond. Process.* **2016**, *50*, 7−13.

(3) Mehta, A.; Mishra, A.; Basu, S.; Shetti, N. P.; Reddy, K. R.; Saleh, T. A.; Aminabhavi, T. M. Band Gap Tuning and Surface Modification of Carbon Dots for Sustainable Environmental Remediation and Photocatalytic Hydrogen Production − A Review. *J. Environ. Manage.* **2019**, *250*, 109486.

(4) Lan, Z.-A.; Fang, Y.; Zhang, Y.; Wang, X. Photocatalytic Oxygen Evolution from Functional Triazine-Based Polymers with Tunable Band Structures. *Angew. Chem., Int. Ed.* **2018**, *57*, 470−474.

(5) Bredas, J.-L. Mind the Gap! *Mater. Horiz* **2014**, *1*, 17−19.

(6) Gindele, F.; Woggon, U.; Langbein, W.; Hvam, J. M.; Leonardi, K.; Hommel, D.; Selke, H. Excitons, Biexcitons, and Phonons in Ultrathin CdSe/ZnSe Quantum Structures. *Phys. Rev. B* **1999**, *60*, 8773−8782.

(7) Chia, C. H.; Yuan, C. T.; Ku, J. T.; Yang, S. L.; Chou, W. C.; Juang, J. Y.; Hsieh, S. Y.; Chiu, K. C.; Hsu, J. S.; Jeng, S. Y. Temperature Dependence of Excitonic Emission in Cubic CdSe Thin Film. *J. Lumin.* **2008**, *128*, 123−128.

(8) Shan, W.; Song, J. J.; Luo, H.; Furdyna, J. K. Determination of the Fundamental and Split-off Band Gaps in Zinc-Blende CdSe by Photomodulation Spectroscopy. *Phys. Rev. B* **1994**, *50*, 8012−8015.

(9) Knupfer, M. Exciton Binding Energies in Organic Semiconductors. *Appl. Phys. A: Mater. Sci. Process.* **2003**, *77*, 623−626.

(10) Kshirsagar, A. R.; Blase, X.; Attaccalite, C.; Poloni, R. Strongly Bound Excitons in Metal−Organic Framework MOF-5: A Many-Body Perturbation Theory Study. *J. Phys. Chem. Lett.* **2021**, *12*, 4045−4051.

(11) Schweitzer, B.; Bässler, H. Excitons in Conjugated Polymers. *Synth. Met.* **2000**, *109*, 1−6.

(12) Hedin, L. New Method for Calculating the One-Particle Green's Function with Application to the Electron-Gas Problem. *Phys. Rev.* **1965**, *139*, A796−A823.

(13) van Setten, M. J.; Weigend, F.; Evers, F. The GW-Method for Quantum Chemistry Applications: Theory and Implementation. *J. Chem. Theory Comput.* **2013**, *9*, 232−246.

(14) Konstantinova, E. A.; Minnekhanov, A. A.; Kokorin, A. I.; Sviridova, T. V.; Sviridov, D. V. Determination of the Energy Levels of Paramagnetic Centers in the Band Gap of Nanostructured Oxide Semiconductors Using EPR Spectroscopy. *J. Phys. Chem. C* **2018**, *122*, 10248−10254.

(15) Bleuse, J.; Perret, S.; Curé, Y.; Grenet, L.; André, R.; Mariette, H. Optical Determination of the Band Gap and Band Tail of Epitaxial $Ag_2ZnSnSe_4$ at Low Temperature. *Phys. Rev. B* **2020**, *102*, 195205.

(16) Klein, P. B.; Nwagwu, U.; Edgar, J. H.; Freitas, J. A. Photoluminescence Investigation of the Indirect Band Gap and Shallow Impurities in Icosahedral $B_{12}As_2$. *J. Appl. Phys.* **2012**, *112*, 013508.

(17) Nandan, Y.; Mehata, M. S. Wavefunction Engineering of Type-I/Type-II Excitons of CdSe/CdS Core-Shell Quantum Dots. *Sci. Rep.* **2019**, *9*, 2.

(18) Cademartiri, L.; Montanari, E.; Calestani, G.; Migliori, A.; Guagliardi, A.; Ozin, G. A. Size-Dependent Extinction Coefficients of PbS Quantum Dots. *J. Am. Chem. Soc.* **2006**, *128*, 10337−10346.

(19) Protesescu, L.; Yakunin, S.; Bodnarchuk, M. I.; Krieg, F.; Caputo, R.; Hendon, C. H.; Yang, R. X.; Walsh, A.; Kovalenko, M. V. Nanocrystals of Cesium Lead Halide Perovskites ($CsPbX_3$, X = Cl, Br, and I): Novel Optoelectronic Materials Showing Bright Emission with Wide Color Gamut. *Nano Lett.* **2015**, *15*, 3692−3696.

(20) Tauc, J. Optical Properties and Electronic Structure of Amorphous Ge and Si. *Mater. Res. Bull.* **1968**, *3*, 37−46.

(21) Mok, T. M.; O'Leary, S. K. The Dependence of the Tauc and Cody Optical Gaps Associated with Hydrogenated Amorphous Silicon on the Film Thickness: Al Experimental Limitations and the Impact of Curvature in the Tauc and Cody Plots. *J. Appl. Phys.* **2007**, *102*, 113525.

(22) Chang, A.-L.; Nguyen, V.-H.; Lin, K.-Y. A.; Hu, C. Selective Synthesis of ZIFs from Zinc and Nickel Nitrate Solution for Photocatalytic H_2O_2 Production. *Arab. J. Chem.* **2020**, *13* (11), 8301−8308.

(23) Wang, T.; Wang, Y.; Sun, M.; Hanif, A.; Wu, H.; Gu, Q.; Ok, Y. S.; Tsang, D. C. W.; Li, J.; Yu, J.; Shang, J. Thermally Treated Zeolitic Imidazolate Framework-8 (ZIF-8) for Visible Light Photocatalytic Degradation of Gaseous Formaldehyde. *Chem. Sci.* **2020**, *11*, 6670−6681.

(24) Pulumati, N. B.; Urs MB, K.; Mandal, S.; Kamble, V. B. Underpinning the Conductivity Mechanism in Wide Bandgap Metal Organic Framework through Chemical Sensing. *AIP Adv.* **2020**, *10*, 085105.

(25) Li, J.; Musho, T.; Bright, J.; Wu, N. Functionalization of a Metal-Organic Framework Semiconductor for Tuned Band Structure and Catalytic Activity. *J. Electrochem. Soc.* **2019**, *166*, H3029.

(26) Taddei, M.; Schukraft, G. M.; Warwick, M. E. A.; Tiana, D.; McPherson, M. J.; Jones, D. R.; Petit, C. Band Gap Modulation in Zirconium-Based Metal−Organic Frameworks by Defect Engineering. *J. Mater. Chem. A* **2019**, *7*, 23781−23786.

(27) Wang, Y. L.; Zhang, S.; Zhao, Y. F.; Bedia, J.; Rodriguez, J. J.; Belver, C. UiO-66-Based Metal Organic Frameworks for the Photodegradation of Acetaminophen under Simulated Solar Irradiation. *J. Environ. Chem. Eng.* **2021**, *9*, 106087.

(28) Hendon, C. H.; Tiana, D.; Fontecave, M.; Sanchez, C.; D'arras, L.; Sassoye, C.; Rozes, L.; Mellot-Draznieks, C.; Walsh, A. Engineering the Optical Response of the Titanium-MIL-125 Metal−Organic Framework through Ligand Functionalization. *J. Am. Chem. Soc.* **2013**, *135*, 10942−10945.

(29) Syzgantseva, M. A.; Stepanov, N. F.; Syzgantseva, O. A. Effect of Ligand Functionalization on the Rate of Charge Carrier Recombination in Metal−Organic Frameworks: A Case Study of MIL-125. *J. Phys. Chem. Lett.* **2021**, *12*, 829−834.

(30) Hlophe, P. V.; Dlamini, L. N. Synthesis of a Semi-Conductor-like MOF with Black Phosphorous as a Composite for Visible Light-Driven Photocatalysis. *RSC Adv.* **2019**, *9*, 37321−37330.

(31) Butler, K. T.; Hendon, C. H.; Walsh, A. Electronic Chemical Potentials of Porous Metal−Organic Frameworks. *J. Am. Chem. Soc.* **2014**, *136*, 2703−2706.

(32) Mancuso, J. L.; Mroz, A. M.; Le, K. N.; Hendon, C. H. Electronic Structure Modeling of Metal−Organic Frameworks. *Chem. Rev.* **2020**, *120*, 8641−8715.

(33) Baerends, E. J.; Gritsenko, O. V.; van Meer, R. The Kohn−Sham Gap, the Fundamental Gap and the Optical Gap: The Physical Meaning of Occupied and Virtual Kohn−Sham Orbital Energies. *Phys. Chem. Chem. Phys.* **2013**, *15*, 16408.

(34) Janesko, B. G.; Henderson, T. M.; Scuseria, G. E. Screened Hybrid Density Functionals for Solid-State Chemistry and Physics. *Phys. Chem. Chem. Phys.* **2009**, *11*, 443−454.

(35) Fabrizio, K.; Lazarou, K. A.; Payne, L. I.; Twight, L. P.; Golledge, S.; Hendon, C. H.; Brozek, C. K. Tunable Band Gaps in MUV-10(M): A Family of Photoredox-Active MOFs with Earth-Abundant Open Metal Sites. *J. Am. Chem. Soc.* **2021**, *143*, 12609−12621.

(36) Kalmutzki, M. J.; Hanikel, N.; Yaghi, O. M. Secondary Building Units as the Turning Point in the Development of the Reticular Chemistry of MOFs. *Sci. Adv.* **2018**, *4*, No. eaat9180.

https://doi.org/10.1021/acsmaterialslett.1c00836
ACS Materials Lett. 2022, 4, 457−463

(37) Furukawa, H.; Cordova, K. E.; O'Keeffe, M.; Yaghi, O. M. The Chemistry and Applications of Metal-Organic Frameworks. *Science* **2013**, *341*, 1230444.
(38) Ding, M.; Flaig, R. W.; Jiang, H.-L.; Yaghi, O. M. Carbon Capture and Conversion Using Metal−Organic Frameworks and MOF-Based Materials. *Chem. Soc. Rev.* **2019**, *48*, 2783−2828.
(39) Vo, T. K.; Kim, J. Facile Synthesis of Magnetic Framework Composite $MgFe_2O_4$@UiO-66(Zr) and Its Applications in the Adsorption−Photocatalytic Degradation of Tetracycline. *Environ. Sci. Pollut. Res.* **2021**, *28*, 68261.
(40) Ding, J.; Yang, Z.; He, C.; Tong, X.; Li, Y.; Niu, X.; Zhang, H. UiO-66(Zr) Coupled with Bi_2MoO_6 as Photocatalyst for Visible-Light Promoted Dye Degradation. *J. Colloid Interface Sci.* **2017**, *497*, 126−133.
(41) Zhou, L.; Liu, F.; Wang, J.; Chen, R.; Chen, Y. Effects of Ligand Functionalization on the Band Gaps and Luminescent Properties of a Zr_{12} Oxo-Cluster Based Metal−Organic Framework. *CrystEngComm* **2021**, *23*, 2961−2967.
(42) Wang, J.; Cherevan, A. S.; Hannecart, C.; Naghdi, S.; Nandan, S. P.; Gupta, T.; Eder, D. Ti-Based MOFs: New Insights on the Impact of Ligand Composition and Hole Scavengers on Stability, Charge Separation and Photocatalytic Hydrogen Evolution. *Appl. Catal. B Environ.* **2021**, *283*, 119626.
(43) Hang, Z.; Yu, H.; Luo, L.; Huai, X. Nanoporous G-C_3N_4/MOF: High-Performance Photoinitiator for UV-Curable Coating. *J. Mater. Sci.* **2019**, *54*, 13959−13972.
(44) Chen, A.; Zhang, J.; Zhou, Y.; Tang, H. Preparation of a Zinc-Based Metal−Organic Framework (MOF-5)/BiOBr Heterojunction for Photodegradation of Rhodamine B. *React. Kinet. Mech. Catal.* **2021**, *134*, 1003−1015.
(45) Mu, X.; Jiang, J.; Chao, F.; Lou, Y.; Chen, J. Ligand Modification of UiO-66 with an Unusual Visible Light Photocatalytic Behavior for RhB Degradation. *Dalton Trans* **2018**, *47*, 1895−1902.
(46) Wang, A.; Zhou, Y.; Wang, Z.; Chen, M.; Sun, L.; Liu, X. Titanium Incorporated with UiO-66(Zr)-Type Metal−Organic Framework (MOF) for Photocatalytic Application. *RSC Adv.* **2016**, *6*, 3671−3679.
(47) Yadav, A.; Panda, D. K.; Zhang, S.; Zhou, W.; Saha, S. Electrically Conductive 3D Metal−Organic Framework Featuring π-Acidic Hexaazatriphenylene Hexacarbonitrile Ligands with Anion−π Interaction and Efficient Charge-Transport Capabilities. *ACS Appl. Mater. Interfaces* **2020**, *12*, 40613−40619.

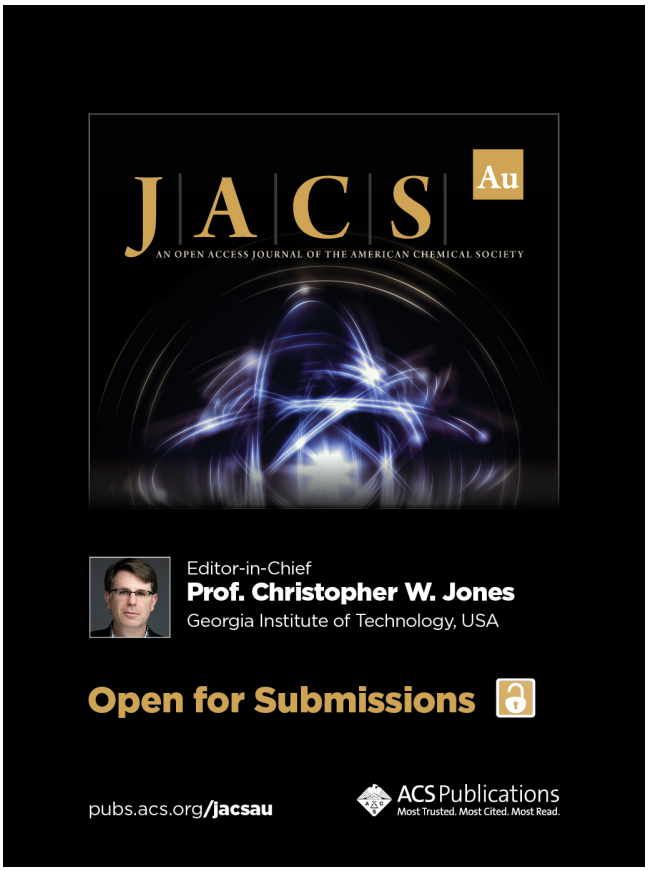

https://doi.org/10.1021/acsmaterialslett.1c00836
ACS Materials Lett. 2022, 4, 457−463